Connective neck evolution and conductance steps in hot point contacts

A. Halbritter,[1] Sz. Csonka,[1] O. Yu. Kolesnychenko,[2] G. Mihály,[1] O. I. Shklyarevskii,[2,3] and H. van Kempen[2]
[1]*Department of Physics, Institute of Physics, Budapest University of Technology and Economics, 1111 Budapest, Hungary*
[2]*Research Institute for Materials, University of Nijmegen, Toernooiveld 1, NL-6525 ED Nijmegen, the Netherlands*
[3]*B. Verkin Institute for Low Temperature Physics & Engineering, National Academy of Science of Ukraine, 47 Lenin Avenue 61164, Kharkov, Ukraine*

(Received 28 May 2001; revised manuscript received 20 September 2001; published 3 January 2002)

Dynamic evolution of the connective neck in Al and Pb mechanically controllable break junctions was studied during continuous approach of electrodes at bias voltages V_b up to a few hundred millivolt. A high level of power dissipation (10^{-4}–10^{-3} W) and high current density ($j \gtrsim 10^{10}$ A/cm^2) in the constriction lead to overheating of the contact area, electromigration, and current-enhanced diffusion of atoms out of the ''hot spot.'' At a low electrode approach rate ($\sim$10–50 pm/s) the transverse dimension of the neck and the conductance of the junction depend on V_b and remain nearly constant over the approach distance of 10–30 nm. For $V_b > 300$ mV the connective neck consists of a few atoms only and the quantum nature of conductance manifests itself in abrupt steps and reversible jumps between two or more levels. These features are related to an ever changing number of individual conductance channels due to the continuous rearrangement in atomic configuration of the neck, the recurring motion of atoms between metastable states, the formation and breaking of isolated one-atom contacts, and the switching between energetically preferable neck geometries.

DOI: 10.1103/PhysRevB.65.045413 PACS number(s): 73.40.Jn, 81.07.−b, 68.35.Fx, 72.15.−v

I. INTRODUCTION

Electron transport through nanometric-sized systems has been a subject of intensive research over the past decade not only because of its obvious technological importance, but primarily due to fascinating effects of fundamental interest related to the quantum nature of the conductance through a few atom metallic contacts.

These phenomena were sought mostly in the single *s*-valence metals using the mechanically controllable break junction (MCBJ) technique in point contacts of submesoscopic size[1–4] and nanowires (long connective necks between the tip and the sample) fabricated using a scanning tunneling microscope (STM).[5–8] More recently this effect was investigated in contacts between two crossed vibrating wires,[9] gold-plated wafer, and gold pin[10] and even in commercial and home-built relays.[11,12] In all these techniques a metallic contact is formed by pressing two electrodes together. During the subsequent separation of the electrodes the conductance decreases in abrupt steps with plateaus, which in some instances are close to integer multiples of the fundamental conductance unit $G_0 = 2e^2/h$.

Individual traces of the conductance vs the electrode displacement $G(z)$ are irreproducible owing to the different dynamical evolution of the connective necks during the break. Statistical analysis of the experimental data includes construction of conductance histograms based on hundreds or even hundreds of thousands of curves.[13] However, with the exception of impressive experiments showing conductance quantization in lithium, sodium, and potassium point contacts,[3,14] the histograms basically reflect the existence of stable neck geometries emerging during the break. This is supported by simultaneous measurements of force and conductance in Au nanowires, demonstrating that jumps in $G(z)$ curves during the deformation of the connective necks are always correlated to mechanical force relaxations and thus, to atomic rearrangements.[15]

Since atomic rearrangement plays a key role, one would expect a perceptible dependence of conductance curves on temperature. Rather surprisingly early STM measurements of Sirvent *et al.*[16] carried out at temperatures of 4, 77, and 300 K produced histograms with practically no difference in shape and position of conductance peaks. On the other hand the only measurements performed on Au and Cu MCBJ at room temperature[4] discovered more prominent structure in the histograms than at 4.2 K. It was explained by the fact that at higher temperatures the connective neck reaches an energetically favorable geometry more easily. This discrepancy might be caused by the high retraction speed of the tip in STM measurements (10^2–10^4 nm/s) which is 4–6 orders of magnitude larger than the electrode approach rate in MCBJ experiments.

Room-temperature measurements with MCBJ impose heavy demands on temperature stability of the setup and require an ultrahigh vacuum environment to avoid contamination or oxidation of freshly broken surfaces. In our experiments, we combined the cleanliness and stability of operating a MCBJ at 4.2 K with sufficient mobility of atoms at the contact area to relax to a low-energy geometry. To this end, we took advantage of the fact that connective necks can be locally overheated at high bias voltages V_b. As the applied voltage drops mainly around the center of the contact within a distance comparable to the contact diameter d, the magnitude of the heating is determined by the ratio between d and the diffusive length for electrons L_i. The latter can be defined as $L_i = \frac{1}{3}\sqrt{l_e l_i}$, where l_e is the elastic mean-free path, and $l_i = v_F \tau_i$ is the inelastic mean-free path of the electron-phonon scattering.[17] If L_i is much smaller than the neck diameter ($L_i \ll d$), the power dissipation takes place in a volume of d^3 around the center of the junction. In the other limiting case ($L_i \gg d$) the power is always dissipated in a

volume of L_i^3 around the junction, regardless of the contact diameter. According to these considerations, and assuming the validity of the Wiedemann-Franz condition, one can make estimations for the temperature of the junction in the different regimes of point contacts. In the thermal limit (l_e, $L_i \ll d$) the temperature in the center of the contact does not depend on d and is given as follows: $T_{\rm pc}^2 = T_{\rm bath}^2 + V_b^2/4\mathcal{L}$, where $\mathcal{L}$ is the Lorentz number.[18] (Or $eV_b \approx 3.63kT_{\rm pc}$ at $T_{\rm bath} = 4.2$ K and high V_b.[17]) Practically it means that a voltage bias of 200–300 mV could heat the contact up to $T_{\rm pc} = 600$–1000 K as it was demonstrated for point contacts between ferromagnetic metals.[19] On the other hand, in the spectroscopic regime (l_e, $L_i \gg d$) the heating of the contact is negligible, and $T_{\rm pc} \approx T_{\rm bath}$. In the intermediate case ($l_e < d < L_i$) simple calculations show that the crossover between the ballistic and thermal limit is mainly determined by the ratio of d and L_i, namely: $T_{\rm pc}^2 = T_{\rm bath}^2 + d/L_i V_b^2/4\mathcal{L}$. Even though in nanometric point-contacts l_e is assumed to be in the range of a few nanometer (due to scattering on defects at the interface of the electrodes), at low temperature and bias voltage L_i remains much larger than the contact diameter due to the large inelastic mean-free path. Therefore, the heating is considerably reduced compared to the thermal limit. However, l_i drops to $\lesssim$10 nm at bias voltage eV_b exceeding the Debye energy of phonons due to the strong electron-phonon coupling. The energy dependence of l_i can be determined from the experimental point-contact spectra of the electron-phonon interaction.[20] The inelastic mean-free path continues to decrease at higher energies due to the relatively large probability of multiphonon scattering.[17] This is in agreement with Ref. 21 where the inelastic mean-free path of a hot electron with excess energy of 100 meV was estimated to be 1–10 nm for most metals. With all the parameters being the same order of magnitude ($L_i \approx l_e \approx d$) it is extremely difficult to give an accurate estimation for the contact temperature, but according to the above considerations contacts of submesoscopic size might be heated well-above room temperature with a voltage bias of a few hundred millivolt.

In this paper, we present conductance curves for Al and Pb point contacts measured at V_b up to 0.4 V using the MCBJ technique, and we give a simple analysis for the observations. These *sp*-like metals are the subject of current interest since the transport properties of one-atom Al or Pb contacts are determined by the existence of *three* conducting channels with nonvanishing transmission and by a strong dependence of the transmission coefficients on the degree of elastic deformation of the neck.[22–26] In the light of recent attempts to study nonlinear effects in conductance in connective necks of a few atoms at eV_b comparable to the Fermi energy[27] the details of the neck evolution at high V_b are of special importance.

II. EXPERIMENT

The basic concepts of MCBJ method were developed by Moreland and Ekin,[28] refined later by Muller and co-authors[29] and described elsewhere.[1–4] In our experiments, we used a slightly modified version of the traditional sample mount presented in the inset in Fig. 1. It includes two additional pieces ($5 \times 3 \times 1$ mm^3) of fiber glass board plate placed underneath the anchoring points of the 200-μm thick polycristalline sample wire. This increases the effective thickness of the bending beam and thus, enlarges the ratio of the electrode displacement Δ_z to the vertical transfer of the piezodriver Δ_y. Such a modification practically does not affect the stability of the break junctions and gives an opportunity to cover the range of Δ_z up to 20–30 nm in one run of the piezodriver.

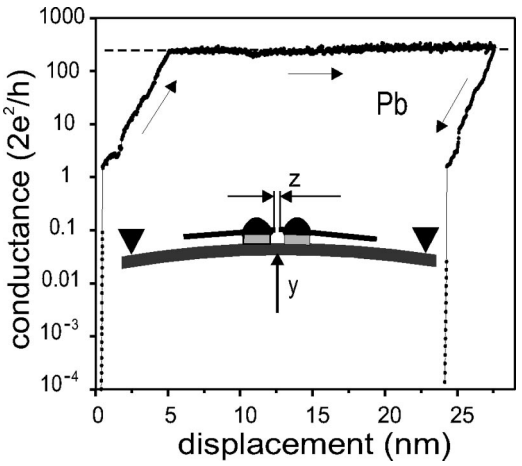

FIG. 1. The conductance of a Pb MCBJ as a function of electrode displacement at a bias voltage of 180 mV. The inset shows the design and the principle of a mechanically controllable break junction (see also text). A bending force causes a vertical displacement *y*, which leads to a displacement *z* between the electrodes. For clarity, all distances have been exaggerated.

Most of the measurements were performed at 4.2 K in He exchange gas at 760 Torr to avoid effects related to thermal expansion of the unglued sections of electrodes. Adsorbtion of He on the electrode surface results in a giant increase of the local work function of metals[30] and a strong deviation of tunnel current vs electrode separation $I(z)$ curve from exponential behavior.[31] As a consequence the standard calibration procedures of the relative displacement of the electrodes [using the $I(z)$ dependence in tunneling regime or field emission resonance spectra[32]] are rather inaccurate. We can estimate Δ_z and the approach rate $S = \Delta_z/t$ with a precision of 25–30%. Fortunately this inaccuracy has little or no effect on our results that are qualitatively the same in a wide range of S from 5 to 50 pm/s.

Contact conductance was measured using a current to voltage converter with a gain of 1 V/mA. Data were recorded with a Keithley 182 nanovoltmeter in a slow (1–10 pt/s) mode and voltage range from 1 μV to 10 V to cover the transition from tunneling to direct conductance. Simultaneously a AT-MIO-16XE-50. National Instruments data acquisition board was used in a fast (250–1000 pt/s) mode in 10 mV–10 V range. Some fragments of conductance curves were measured at the rate of 10 000 pt/sec for 1–2 min.

All results presented below are based on a careful analysis of a few hundreds $G(z)$ traces obtained on 5–6 different samples for each metal.

III. RESULTS AND DISCUSSION

In this section, we present experiments on locally overheated Pb and Al MCBJ. In the low bias voltage measurements ($V_b \approx 10\,\mathrm{mV}$) the conductance of the contacts increases monotonically while the electrodes are continuously pushed together by the piezodriver. At elevated bias voltages the conductance grows only to a certain value (determined mainly by the magnitude of V_b) and, thereafter, saturates at a constant level during subsequent electrode approaches as large as 20 nm. This part of the conductance curve, where the fluctuations are caused by temperature and current induced atomic rearrangements, can be analyzed with histograms based on a *single* sweep of the electrode approach. Furthermore, with fast data acquisition one can get an insight into the dynamics of thermally activated point contacts.

A typical conductance curve for a Pb MCBJ recorded at an approach rate of approximately 0.01 nm/s and a bias voltage of 180 mV is presented in Fig. 1. After the transition from tunneling to direct contact the conductance of the connective neck increases reaching $G \approx 250-300\ G_0$ and subsequently remains nearly constant (or rises very slowly) during further electrode approaches over a distance of $\sim$22 nm. Retracting the electrodes back to the tunneling range reveals an increase of $\sim$24 nm in electrode separation with respect to their initial position. This indicates irreversible changes in the electrode relief (reduction of electrode length) caused by continuous transfer of atoms from the neck area to more remote parts of the electrode. In our opinion two mechanisms are responsible for the effect observed.

(i). Surface diffusion of atoms: the high level of power dissipation (up to $10^{-3}\,\mathrm{W}$) in the region with characteristic dimension of L_i around the contact raises the neck temperature and, therefore, the atomic diffusion. This induces motion of atoms from the ''hot spot'' in the center of the connective neck to colder areas of the electrodes.

(ii). Electromigration of atoms: the estimated current density in the center of the point-contact presented in Fig. 1 is $j \sim 10^{10}\,\mathrm{A/cm^2}$. At such current densities the electron wind forces resulting from the scattering of electrons on lattice defects are $F_{\mathrm{ew}} \approx 0.1-0.2\,\mathrm{nN}$.[11,33] These current-induced forces are one order of magnitude too small to break bonds between atoms but are able to enhance diffusion and make atomic flux directional causing a preferential transfer of atoms to one of the electrodes. Breaking of gold nanowires caused by electromigration of atoms at $V_b \approx 300-500\,\mathrm{mV}$ was reported recently by Park *et al.*[34]

The neck conductance remains nearly constant because of a peculiar ''feedback'' of natural origin. In a voltage-biased measurement the increase of contact diameter in the course of electrode approach leads to an increase of G and power dissipation. At $L_i \gtrsim d$ the volume where this power is dissipated remains the same ($\sim L_i^3$), thus the temperature increases, causing an exponential increase of diffusion. Thus, the number of atoms leaving the neck area per unit of time increases and the diameter is reduced back.

At higher bias ($V_b \approx 250-300\,\mathrm{nV}$) the contact conductance saturates already at $40-80\ G_0$. An example of the flat part for such a $G(z)$ dependence is presented in Fig. 2(a)

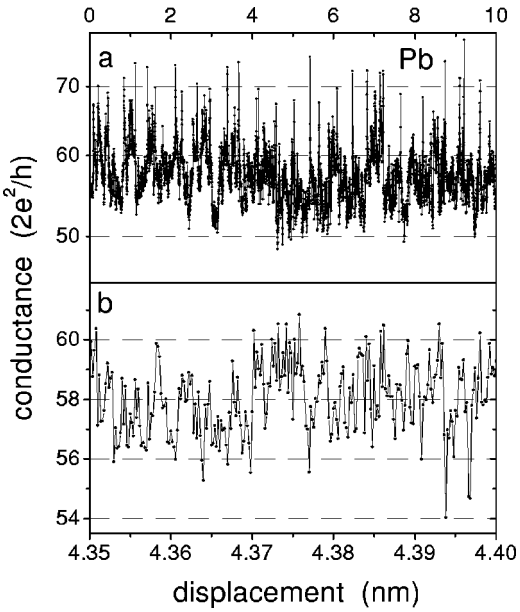

FIG. 2. (a) $G(z)$ dependence for Pb MCBJ recorded at $V_b = 280\,\mathrm{mV}$ and approach rate $S = 40\,\mathrm{pm/s}$ (only 5% of measured points are plotted). (b) A part of the $G(z)$ trace in the upper panel presented on an extended scale.

(with no more than 5% of the experimental points plotted) and a fragment of this curve is shown on an extended scale in Fig. 2(b). The random changes in the conductance are caused by a continuous rearrangement of atoms in the neck area. Halting of the electrode approach eventually reduces the amplitude of G variations by a factor of $\approx$3–10. The mean value of G remains practically the same or slightly decreases. The conductance does not relax to a lower value since at extremely slow approach rate the system is already in a quasiequilibrium state. An increase of bias voltage for stationary contact reduces the conductance, whereas a decrease leaves the conductance unchanged as no diffusion to the overheated neck area from the colder part of electrodes can occur. (The former effect imposes a limitation on measurements of current-voltage dependencies.[35]) It should be noted, though, that power dissipation in this contact (proportional to $V_b^2 G$) is $\approx$2 times less than in the previous case (Fig. 1), whereas current density increases. Although it is very difficult to make any reasonable estimation for the connective-neck temperature in this intermediate ''diffusive'' range, it may be safely suggested that the contribution of the current-induced processes in neck evolution increases with increasing bias voltage.

The conductance histogram for this scan is presented in [Fig. 3(a)] and is nearly Gaussian shaped. It is slightly cut at the low conductance end and extended to larger G. The histogram plot for the *difference* in conductance between the neighboring data points $\Delta G = G_{n+1} - G_n$ for the same scan is shown in Fig. 3(b). The significance of this type of histogram for data analysis will become clear later. At this point it simply demonstrates that on the time scale of the data acquisition (1 ms) no preferential values of ΔG are observed. As the conductance of a point contact is mainly determined by a volume of d^3 around the contact center, hundreds of atoms

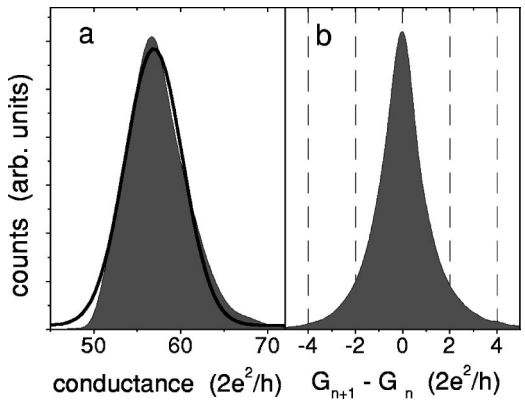

FIG. 3. (a) Conductance histogram and Gaussian fit (solid line) for the $G(z)$ curve presented in Figs. 2(a). (b) Histogram plot of conductance difference between neighboring points $G_{n+1}-G_n$ for the same curve.

are responsible for the resistance of this junction. The classical continuous spectrum demonstrated by both figures is not surprising, as the number of different metastable atomic configurations is so large, that they can hardly be resolved as distinct peaks in conductance histograms. Or speaking in terms of conductance channels, for contacts of the above size the spacing between the energies of different channels is so small that it can easily be smeared either by temperature or by the enhanced scattering inside the contact.

At V_b as high as 300–400 mV the neck conductance is restricted to 10–20 quantum units over 10–15 nm of electrode approach. In this case the power dissipated in the electrodes, is 5 to 10 times less than that for point contact presented in Fig. 1. Moreover, contacts of such dimension ($\sim$1 nm) are quasiballistic, thus no significant power dissipation takes place in the nearest vicinity of connective neck. At the same time the current density nears 10^{11} A/cm^2, greatly increasing the contribution of electromigration and current-enhanced diffusion to the neck evolution. Typical $G(z)$ dependencies are presented in Fig. 4 for Al and Pb MCBJ. Again only 1–3% of all recorded points are plotted for the sake of better clarity, as the total number of different neck configurations measured per one scan reaches $\sim 10^5$. Both curves show a pronounced steplike structure and clear cut recurring jumps of neck conductance between two or more levels. In the following, we concentrate on these phenomena.

Just as usual conductance curves these $G(z)$ dependencies are inherently irreproducible for different samples since their behavior is determined by fine details of ill-controllable surface relief of the electrodes. The general shape of $G(z)$ curves does not depend appreciably on the approach rate S in the 5 to 50 pm/s range. An increase of S above 100 pm/s produces effects similar to a decrease of V_b. At $S \gtrsim 1$ nm/s conductance curves assume the standard low bias behavior: monotonous increase in G up to $10^4 G_0$. This shows that in reality the process of atomic rearrangements in the connective neck (even at elevated temperature) could be many orders of magnitude slower than it was suggested in molecular-dynamic simulations.[36] Thus, it is hardly surprising that in experiments with gold relays[11] at approach rates of $\gtrsim 10^5$ nm/s the authors did not find any difference between

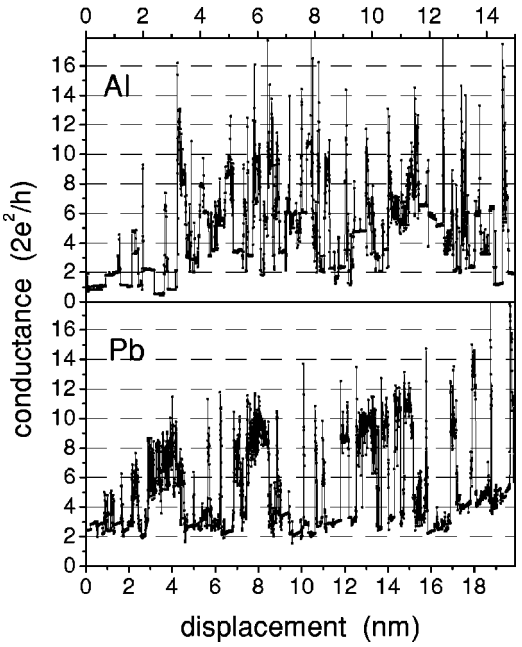

FIG. 4. $G(z)$ dependencies for Al (recorded at $V_b = 340$ mV and $S = 40$ pm/s) and for Pb (recorded at $V_b = 360$ mV and $S = 30$ pm/s) in quantum regime of conductance.

conductance histograms taken at low V_b and bias voltage as high as 500 mV and observed a plateau in conductance curves corresponding to the one-atom contacts even at $V_b = 1.5$ V. Contrary to this, in experiments with Au (as well as Al and Pb) MCBJ, we were unable to create one-atom contact already at $V_b \geqslant 0.8-1.0$ V and $S \sim 0.01$ nm due to field desorption or field evaporation of the surface atoms at small interelectrode distances.

Figure 5 presents a histogram plot for Al MCBJ based on

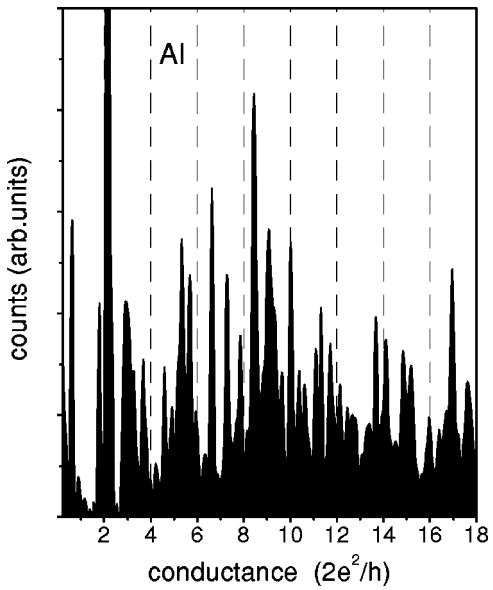

FIG. 5. Conductance histogram for Al corresponding to more than 10^5 individual neck configurations. The raw data were smoothed with a narrow window of 0.1 G_0. The original $G(z)$ curve was recorded at $V_b = 350$ mV and $S = 30$ pm/s.

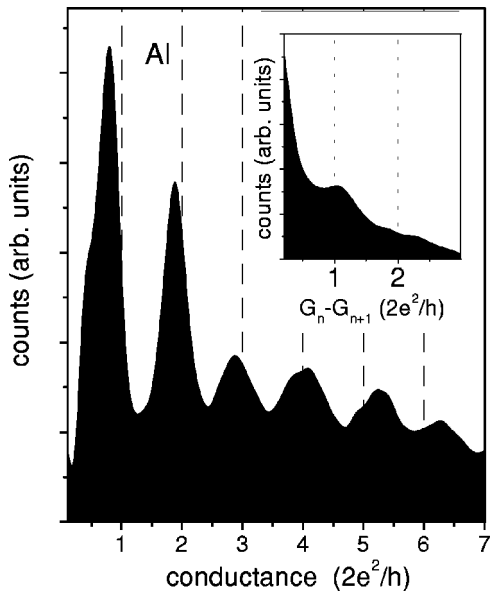

FIG. 6. Low bias conductance histogram for Al MCBJ based on 5000 individual traces recorded at 100 mV bias. Inset: differential histogram for the same set of data displaying a peak around 1.1 G_0.

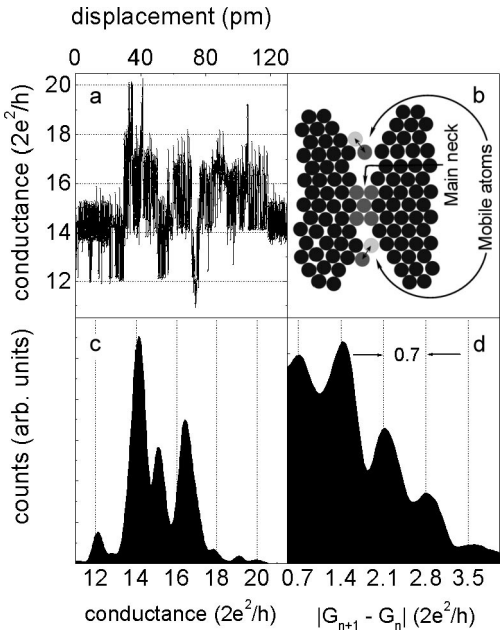

FIG. 7. (a) A fragment of a $G(z)$ dependence for Al ($V_b = 340$ mV and $S = 50$ pm/s); (b) model of formation and break of the single-atom contacts being separated from the main neck and from each other; (c) Histogram plot for the conductance curve (a); and (d) histogram plot for the absolute value of the conductance difference ΔG between neighboring points of curve (a) demonstrating a succession of maxima separated by $\sim 0.7\ G_0$;

more than 10^5 of different connective-neck configurations recorded in a single 20 nm scan. It displays a number of well-defined peaks in the range from 0.5 to $18G_0$. The total conductance of a contact with few atoms is determined by the sum of N independent conducting channels with their respective transmission coefficients $G = G_0 \Sigma_{i=1}^{N} \tau_i$. Rearrangement of atomic positions may result in a completely different transmission set $\mathbb{T} = \Sigma_{i=1}^{N} \tau_i$ for the whole neck.[22] Data presented in Fig. 5 clearly show that in the course of continuous neck evolution under elevated temperature and high current density the selection of the most stable neck geometries occurs. Only the preferable (energetically favorable) atomic arrangements can survive for a long enough time to give a rise to the sharp peaks in the histogram.

In Al and Pb contacts the $G(z)$ dependencies are especially sensitive to the elastic deformation of the connective neck in the process of creation and break of contacts at low bias voltage.[25,26] This is reflected as a steep slope of plateaus in the conductance staircase and causes a considerable smearing of the peaks in the histograms. An example of a conventional histogram for Al based on 5000 individual $G(z)$ traces measured at low bias voltage is presented in Fig. 6. (We did not find any perceptible difference in peak positions for histograms taken at low bias voltages and at 300 mV. This indicates a rather small nonlinearity of I–V characteristics of a few atom Al MCBJ.) At high V_b and a slow approach of electrodes the deformation of the neck is much moderate because of a fast relaxation of strain through diffusion of atoms and electromigration of defects. For this reason the plateaus in our conductance curves (Fig. 4) are tilted less than in $G(z)$ curves recorded at low bias.[25]

We performed further analysis of the dynamic evolution of contacts with conductance restricted by 20–25 quantum units using selected fragments typical for most of the conductance curves. An example is presented in Fig. 7(a). The contact conductance switches between a few preferential levels, though we did not find any regular trend in the peak positions in the traditional histogram plot [Fig. 7(c)]. At the same time the histogram for the difference of conductance between neighboring data points $\Delta G = |G_{n+1}(z) - G_n(z)|$ demonstrates the succession of 4–5 maxima separated by $0.7G_0$ [Fig. 7(d)]. Since the value of $0.7G_0$ is very close to the experimentally measured[14] and calculated[25] conductivity through a one-atom Al contact for an undistorted lattice, it is reasonable to relate this unexpected periodicity to variations in the number of atoms in the connective cross section by $\pm 1, \ldots, \pm 5$ during the time between successive measurements (1 ms). However, in traditional histograms, based on thousands of conductance traces no such periodicity was observed, and the separation between peaks is much larger ($1.1G_0$). This means that the conductance of a single neck with n atoms in the cross section is not simply the sum of n one-atom contacts. The observed effect is most likely related to momentary formation and breaking of one-atom contacts isolated from the main neck. Due to surface roughness at the atomic scale two electrodes can be bridged for a short time by mobile atoms moving along the surface [see model, in Fig. 7(b)]. The conductance of parallel connected one-atom contacts separated both from each other and from the main neck is simply given as a sum of the conductance of the individual contacts, which explains the periodicity of the peaks in the histogram plot in Fig. 7(d). It should be emphasized that the visual appearance of this histogram plot probably depends on the recording rate: an increase in this will leave us finally with a sole peak at $0.7G_0$ corresponding to

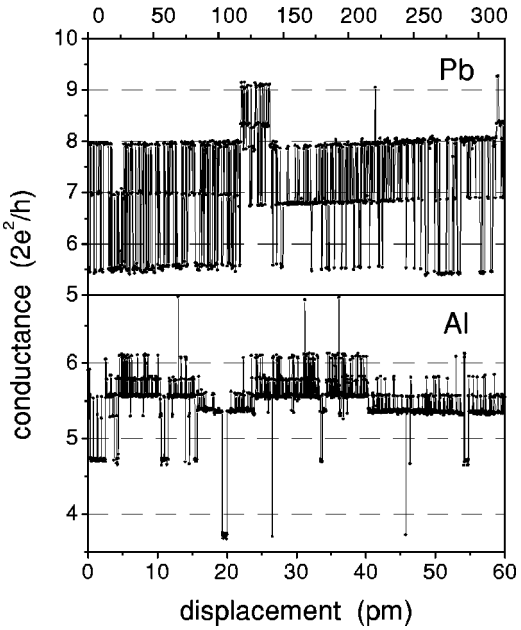

FIG. 8. Short fragments of conductance curves for Al ($V_b = 350$ mV and $S = 30$ pm/s) and Pb ($V_b = 360$ mV and $S = 30$ pm/s) demonstrating random telegraph noise patterns corresponding to fluctuation of atoms between two metastable states accompanied by creation (rupture) of one-atom point contacts. Conductance jumps of smaller amplitude corresponds to changes in the number of conducting channels due to incomplete overlap of orbitals.

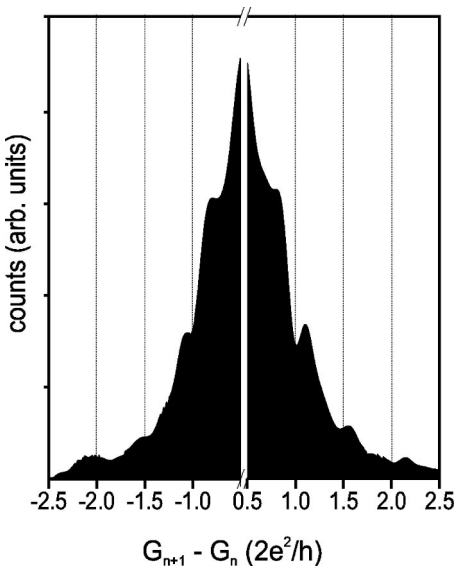

FIG. 9. Differential histogram for Al MCBJ demonstrating singularities caused by formation and break of one-atom contacts and by transitions between the stable configurations of the neck (see text).

the creation or break of a single one-atom contact between two successive measurements. At the same time the possibility of simultaneous formation of two or more one-atom contacts in a single event cannot be ruled out. This result opens an interesting possibility to study the dynamics of single-atom contact formation under different circumstances by extending the time scale of data recording into microseconds range.

Yet another two typical fragments of conductance curves for Pb and Al MCBJ with somewhat lower conductance are presented in Fig. 8. They exhibit typical random telegraph noise behavior observed on many occasions in different mesoscopic systems. In our case these fluctuations between discrete levels are caused by switching of Al or Pb atoms between metastable positions. In both cases the repeatable jumps with larger amplitude ($0.8G_0$ for Al, and $2.4G_0$ for Pb) might correspond to the formation and break of isolated one-atom contacts [the calculated conductivity through a one-atom Pb contact is $\approx 2.5G_0$ (Refs. 24, 25)]. The above transitions are alternating with conductance jumps of lesser amplitude: $\Delta G = 1.1G_0$ for Pb and $\Delta G = 0.5G_0$ and $0.2G_0$ for Al. These additional two-level transitions can be explained by the recurring motion of atoms comprising the one-atom contact, which only slightly alternates their relative positions. The conducting channels in single-atom contacts of polyvalent metals are generally associated with atomic orbitals.[25] In the case of different orientation and spatial extent of orbitals (which is not improbable for atoms at a metal-vacuum interface) a small displacement of atoms can change the overlapping of electron densities associated with different orbitals and, therefore, induce the complete shut down of certain channels. For instance, the transition with ΔG of 0.5 and $0.2G_0$ in Al may be linked to the switching off and on of high transmissive sp_z or low transmissive $p_{x,y}$ channels, respectively, while the transitions with $\Delta G \approx 1.1G_0$ in Pb are close to conductance through one of the three conductive channels.[24,25] Thus, the transitions of smaller amplitude in Fig. 8 might be related to changes in the *number* of conducting channels through parallel connected one-atom contact.

To be certain that the above effects are not related only to selected fragments of conductance curves, we build up differential histograms for complete scans with a large number ($\sim 10^5$) of different connective-neck configurations. These histograms (Fig. 9) for Al MCBJ show shoulders or smeared peaks at $0.6-0.8G_0$, around $1.5G_0$ and sometimes even at $2.0-2.2G_0$ corresponding to the formation and break of one or more single-atom contacts separated from the main neck. A comparison to Fig. 7 reveals an additional peak at $\approx 1.1G_0$ that means that transitions with $\Delta G = 1.1G_0$ are also preferable. Analysis of the traditional conduction histograms (as the one presented in Fig. 6) shows that the separation between two-neighboring peaks (or statistically more favorable neck configurations) is indeed very close to $1.1G_0$ (this fact was mentioned in Ref. 14 as well). This is further supported by the peak at $1.1G_0$ in the differential histogram for the same data set of 5000 individual conductance curves (see, inset in Fig. 6). Although the reason for nearly equidistant spacing of peaks in Al conductance histograms is not yet clear, one can state that the conductance difference between the stable configurations of a small neck is approximately $1.1G_0$. The peak at $1.1G_0$ in Fig. 9 might also reflect the switching between the stable geometries of the main neck, while the rest of the peaks come from the formation and breaking of isolated one-atom contacts and not expected in

the traditional low bias voltage histogram.

To summarize briefly, in the connective necks with conductivity in the range below $20G_0$ the superposition of the following effects have been seen: switching between the favorable neck configurations (leading to a $\Delta G = 1.1G_0$ peak in differential histograms for Al MCBJ); connecting and disconnecting of one-atom contacts separated from the main neck (which are resulting in a conductivity jump of $0.7G_0$ in Al and $2.5G_0$ in Pb MCBJ); switching ''on'' and ''off'' the individual conductive channels associated with atomic orbitals in the one-atom contacts (conductance jumps on a smaller scale).

The increase of V_b above 400 mV results in unstable behavior of Al contacts with frequent disconnection of electrodes (jumps to tunneling and back). On many occasions, we were able to maintain contacts of one atom over the approach distance up to 2–3 nm. The histogram for such conductance curves mostly reveals ''fine structure'' of the first peak—splitting into two clearly cut components [Fig. 10(a)]. To explain this effect one may consider switching of the one-atom neck between two different well-defined and stable configuration that are incorporating the adjacent atoms of both electrodes (e.g., bent and straight necks connecting two Al electrodes are supposed to have a different conductance[26]). In conventional low bias conductance histograms for Al the first peak is rather broad and centered around $0.8G_0$. However, we found that on rare occasions it has a low-energy ''shoulder'' or can even be split [see Fig. 10(b)], indicating that the contact break may occur in two different ways.

Concluding, we used a method for investigation of connective-neck evolution, based on the fact that at elevated bias voltages and slow approach of the electrodes the conductance of the constriction remains within a limited range over a relatively long distance of electrode displacement due to the current-enhanced diffusion and electromigration of atoms out of the overheated area. The dynamics of neck evolution can be traced using $G(z)$ dependencies and a differential histogram technique. For conductances higher than $\sim 50G_0$ the fluctuation of $G(z)$ demonstrates a quasiclassical continuous spectrum. In the range up to 20 fundamental units

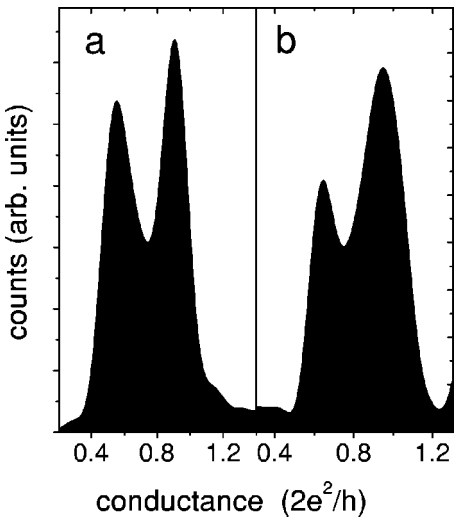

FIG. 10. ''Fine structure'' of the first peak in conductance histograms for Al one-atom contacts. (a) Histogram made during continuous approach ($V_b = 400$ mV and $S = 30$ pm/s). (b) Conventional histogram based on 5000 $G(z)$ curves recorded at 100 mV bias.

the quantum nature of conductance shows up in a discrete spectrum due to an ever changing number of individual conductance channels, continuous formation and rupture of parallel connected one-atom contacts isolated from the main neck and transition between preferable neck geometries. The dependence of the $G(z)$ traces on the approach rate shows that the relaxation of atoms in the connective neck occurs much slower than it had been suspected before.

ACKNOWLEDGMENTS

We are indebted to I. K. Yanson for stimulating discussions. Part of this work was supported by the Stichting voor Fundamenteel Onderzoek der Materie (FOM) which is financially supported by the Netherlands Organization for Scientific research (NWO), the Hungarian Research Funds OTKA T026327 and N31769 and a NWO grant for Dutch-Hungarian cooperation. O. I. S. wishes to acknowledge the NWO for a visitor's grant.

[1] C. J. Muller, J. M. van Ruitenbeek, and L. J. de Jongh, Phys. Rev. Lett. **69**, 140 (1992).
[2] J. M. Krans and J. M. van Ruitenbeek, Phys. Rev. B **50**, 17 659 (1994).
[3] J. M. Krans, J. M. van Ruitenbeek, V. V. Fisun, I. K. Yanson, and L. J. de Jongh, Nature (London) **375**, 767 (1995).
[4] C. J. Muller, J. M. Krans, T. N. Todorov, and M. A. Reed, Phys. Rev. B **53**, 1022 (1996).
[5] J. I. Pascual, J. Mendez, J. Gomez-Herrero, A. M. Baro, N. García, and Vu Thien Binh, Phys. Rev. Lett. **71**, 1852 (1993).
[6] N. Agraït, J. G. Rodrigo, C. Sirvent, and S. Vieira, Phys. Rev. B **48**, 8499 (1993).
[7] L. Olesen, E. Lægsgaard, I. Stensgaard, F. Besenbacher, J. Schiotz, P. Stoltze, K. W. Jacobsen, and J. K. Nørskov, Phys. Rev. Lett. **72**, 2251 (1994).
[8] C. Untiedt, G. Rubio, S. Vieira, and N. Agrait, Phys. Rev. B **56**, 2154 (1997).
[9] J. L. Costa-Krämer, N. García, P. García-Mochales, P. A. Serena, M. I. Marqués, and A. Correia, Phys. Rev. B **55**, 5416 (1997).
[10] U. Landman, W. D. Luedtke, B. E. Salisbury, and R. L. Whetten, Phys. Rev. Lett. **77**, 1362 (1996).
[11] H. Yasuda and A. Sakai, Phys. Rev. B **56**, 1069 (1997).
[12] K. Hansen, E. Lægsgaard, I. Stensgaard, and F. Besenbacher, Phys. Rev. B **56**, 2208 (1997).
[13] J. L. Costa-Krämer, N. García, and H. Olin, Phys. Rev. B **55**, 12 910 (1997).

[14] A. I. Yanson, Ph.D. thesis, University of Leiden, 2001.
[15] G. Rubio, N. Agraït, and S. Vieira, Phys. Rev. Lett. **76**, 2302 (1995).
[16] C. Sirvent, J. G. Rodrigo, N. Agraït, and S. Vieira, Physica B **218**, 238 (1996).
[17] I. K. Yanson and O. I. Shklyarevskii, Sov. J. Low Temp. Phys. **12**, 509 (1986).
[18] R. Holm, *Electric Contacts* (Springer Verlag, Berlin, 1967).
[19] B. I. Verkin, I. K. Yanson, I. O. Kulik, O. I. Shklyarevskii, A. A. Lysykh, and Yu. G. Naydyuk, Solid State Commun. **30**, 215 (1979).
[20] I. K. Yanson, and A. V. Khotkevich *Atlas of Point-Contact Spectra of Electron-Phonon Interaction in Metals* (Naukova Dumka, Kiev, 1986).
[21] B. N. J. Persson and J. E. Demuth, Solid State Commun. **57**, 769 (1986).
[22] E. Scheer, P. Joyez, D. Esteve, C. Urbina, and M. H. Devoret, Phys. Rev. Lett. **78**, 3535 (1997).
[23] J. C. Cuevas, A. Levy Yeyati, and A. Martín-Rodero, Phys. Rev. Lett. **80**, 1066 (1998).
[24] E. Scheer, N. Agraït, J. C. Cuevas, A. Levy Yeyati, B. Ludoph, A. Martín-Rodero, G. Rubio Bollinger, J. M. van Ruitenbeek, and C. Urbina, Nature (London) **394**, 154 (1998).
[25] J. C. Cuevas, A. Levy Yeyati, A. Martín-Rodoro, G. Rubio Bollinger, C. Untiedt, and N. Agraït, Phys. Rev. Lett. **81**, 2990 (1998).
[26] N. Kobayashi, M. Brandbyge, and M. Tsukada, Phys. Rev. B **62**, 8430 (2000).
[27] K. Itakura, K. Yuki, S. Kurokawa, H. Yasuda, and A. Sakai, Phys. Rev. B **60**, 11163 (1999).
[28] J. Moreland and J. W. Ekin, J. Appl. Phys. **58**, 3888 (1985).
[29] C. J. Muller, J. M. van Ruitenbeek, and L. J. de Jongh, Physica C **191**, 485 (1992).
[30] O. Yu. Kolesnychenko, O. I. Shklyarevskii, and H. van Kempen, Phys. Rev. Lett. **83**, 2242 (1999).
[31] R. J. P. Keijsers, J. Voets, O. I. Shklyarevskii, and H. van Kempen, Phys. Rev. Lett. **76**, 1138 (1996).
[32] O. Yu. Kolesnychenko, O. I. Shklyarevskii, and H. van Kempen, Rev. Sci. Instrum. **70**, 1442 (1999).
[33] T. Schmidt, R. Martel, R. L. Sandstrom, and P. Avouris, Appl. Phys. Lett. **73**, 2173 (1998).
[34] H. Park, A. K. L. Lin, A. P. Alivisatos, J. Park, and P. L. McEuen, Appl. Phys. Lett. **75**, 301 (1999).
[35] Typically the upper voltage limit of I–V curves for Al MCBJ, attainable without irreversible changes in conductivity is $\lesssim$200 mV for contact with $G \approx 100-200\ G_0$. It increases up to 250–300 mV for $G \approx 30-100\ G_0$, reaches 350–400 mV for G in the range $10-30\ G_0$ and peaks at 500–600 mV for the stable contact configurations with conductivity less than $10\ G_0$. In all cases the relative change of conductivity at the highest V_b with respect to zero bias conductivity was $\lesssim$3–5 % and, therefore, the nonlinearity of I–V curves has little effect on our data.
[36] A. M. Bratkovsky, A. P. Sutton, and T. N. Todorov, Phys. Rev. B **52**, 5036 (1995).